

Identification of PI3K α inhibitors through pharmacophore design and drug repositioning

Paolo Wong Chero ^{1,a}; Daniel Ramírez Lupuche ^{1,b}; Richard Zapata Dongo ^{1,c}; Brenda Moy Díaz ^{1,d}; Stefany Infante Varillas ^{1,e}; Juan Faya Castillo* ^{1,f}

ABSTRACT

Objective: Phosphatidylinositol 3-kinase (PI3K) is one of the most frequently mutated proteins in cancer, resulting in changes to its roles in regulating metabolism, immunity and other cellular functions. Despite the identification of specific drugs targeting PI3K, significant resistance to these therapies has been observed. Therefore, the search for new inhibitors is crucial. This project proposes a strategy based on in silico tools for screening Food and Drug Administration (FDA)-approved drugs, aiming to evaluate their potential for drug repositioning.

Materials and methods: This study obtained the sequence of PI3K α from UniProt Knowledgebase and its three-dimensional structure from AlphaFold Protein Structure Database, which were then coupled with adenosine triphosphate (ATP) and its selective inhibitors: inavolisib, taselisib, CH5132799, alpelisib and ZSTK474. Drug-protein interaction analysis was performed using Protein-Ligand Interaction Profiler (PLIP) and its visualization was done in PyMOL. Based on this information, pharmacophores were generated as models for virtual screening using the FDA-approved drug library available in Pharmit (<https://pharmit.csb.pitt.edu/search.html>).

Results: Key atomistic positions of drug-protein interactions were identified based on the selective PI3K α inhibitors interaction, leading to the generation of nine pharmacophores. A virtual screening resulted in 22 drugs that met the proposed criteria, out of which 10 had binding energy values (kcal/mol) equal to or higher than those of the PI3K α inhibitors. Subsequently, three drugs with potential use for drug repositioning were selected.

Conclusions: This study proposes fostamatinib, pralatrexate and entecavir as potential candidates for drug repositioning. Additionally, the nine pharmacophores can be utilized in other drug databases for identifying new molecules and/or drugs with potential for drug repositioning. Further in silico and in vitro studies of the proposed drugs are recommended.

Keywords: PI-3K, Molecular Docking Simulation; Computational Biology; Neoplasms; Pharmacophore (Source: MeSH NLM).

INTRODUCTION

The significant pathological variability of cancer and its growing drug resistance are increasingly limiting the efficacy of many treatments and worsening patient prognosis ⁽¹⁾. In the search for new therapeutic strategies to address these challenges, several studies have focused on the metabolic pathways involved in cancer development and progression to identify potential points of metabolic inhibition and halt tumor growth. Among these potential targets is phosphatidylinositol 3-kinase (PI3K), a key enzyme for regulating metabolism, immunity and other cellular functions. Notably, PIK3CA is one of the most frequently mutated genes in cancer, with alterations detected in approximately 14 % of all cases. Consequently, PI3K-targeted drugs have been developed in recent years ⁽¹⁻³⁾. Pan-PI3K inhibitors are expected to help overcome cancer resistance to a wide variety of therapies such as chemotherapy, radiation and targeted therapies ^(4,5).

PI3K is a family of lipid kinases categorized into three classes: I, II and III, with class I further subdivided into subtypes A and B ⁽⁶⁾. These kinases act as signal transducers of receptor tyrosine kinases (RTKs), G protein-coupled receptors (GPCRs) and GTPases, ultimately regulating various cellular processes such as growth, proliferation, differentiation, migration, motility and apoptosis ^(1,2). Class IA PI3K consists of a p85 regulatory subunit (p85 α , p85B, p55 α , p55 γ , p50 α) and a p110 catalytic subunit (p110 α , p110B, p110 γ , p110 δ) ⁽⁶⁾. The p110 catalytic subunit consists of an adaptor-binding domain (ABP), a RAS-binding domain (RBD), a membrane-binding C2 domain (C2), a helical domain, and a C-terminal catalytic domain (N- and C-terminal sections), which includes the hinge region where adenosine triphosphate (ATP) binds ⁽²⁾. Meanwhile, the p85 regulatory subunit is composed of the SRC homology 3 (SH3) domain, breakpoint cluster region-homology (BH) domain, and internal SH2 (iSH2), C-terminal SH2 (cSH2) and N-terminal SH2 (nSH2) domains,

¹ Universidad de Piura, School of Human Medicine, Lima, Peru.

^a Doctor of Medicine, master's degree in Biomedical Research; ^b Human Medicine student; ^c Biologist, master's degree in Biomedical Research;

^d Pharmaceutical chemist; ^e Microbiologist, master's degree in Biomedical Research; ^f Biologist, master's degree in Bioinformatics.

*Corresponding author.

which must dissociate from the p110 subunit to activate PI3K⁽⁴⁾. Oncogenic mutations in PI3K are primarily found in the p110 catalytic subunit, specifically within RBD, helical (E542K, E545K) and catalytic (H1047R) domains⁽⁷⁾. These somatic mutations promote a gain of function, leading to excessive PI3K activity⁽⁴⁾ and enhancing activation mechanisms between p110 and p85⁽²⁾. Notably, studies have shown that eliminating PI3K activity halts tumor growth⁽⁸⁾.

Based on the structural characterization of PI3K and its cytostatic effect upon inhibition, drugs have been developed to achieve tumor stabilization⁽²⁾. These drugs are generally ATP-competitive inhibitors and can be classified into pan-inhibitors, isoform-selective inhibitors and dual PI3K/mTOR inhibitors⁽⁶⁾. The first developed pan-inhibitors were wortmannin and LY294002^(9,10). Later, in 2014, idelalisib (PI3K δ inhibitor) became the first approved PI3K inhibitor⁽²⁾. To date, five PI3K inhibitors have been approved by the Food and Drug Administration (FDA): copanlisib, idelalisib, umbralisib, duvelisib and alpelisib⁽⁶⁾. Despite these advancements, some challenges have hindered clinical trials and drug approval, such as poor tolerance to pan-inhibitors and dual PI3K α /PI3K δ inhibitors, intrinsic and acquired drug resistance, and signaling feedback loops that neutralize PI3K inhibition⁽²⁾. Additionally, achieving isoform selectivity remains difficult, as even currently approved inhibitors can affect multiple PI3K isoform in clinical settings⁽²⁾.

Cancer resistance to PI3K inhibitors arises through various mechanisms, including PI3K mutations and amplification, drug toxicity, positive feedback leading to compensatory mechanisms, non-coding ribonucleic acid (RNA) regulation of PI3K signaling, increased insulin production, and other miscellaneous mechanisms⁽⁶⁾. These challenges, along with the low isoform selectivity, have driven the search for novel therapeutic strategies. This study employs *in silico* drug repositioning techniques to identify FDA-approved drugs with potential PI3K inhibitory activity, despite their original indications⁽¹¹⁾. A computational approach was used to rapidly screen for competitive PI3K inhibitors based on nine different pharmacophore models. This method provides a cost-effective and rapid strategy for identifying candidate drugs while leveraging their well-established safety profiles from preclinical and clinical studies required for approval⁽¹¹⁾.

MATERIALS AND METHODS

Study design and population

This descriptive study was conducted using *in silico* assays in the laboratories at Universidad de Piura. The *in silico* analyses employed specialized bioinformatics approaches and tools, with the catalytic domain of PI3K serving as the

study population. To obtain the structure of PI3K α (p110), the UniProt Knowledgebase (code: P42336) was initially used as a reference, since the crystallized structures available in Research Collaboratory for Structural Bioinformatics Protein Data Bank (RCSB PDB) (www.rcsb.org) were incomplete. The final model of the catalytic domain of PI3K α was retrieved from AlphaFold Protein Structure Database (<https://alphafold.ebi.ac.uk/>), which provides high-confidence predictions.

PI3K α inhibitors were identified from the literature and their co-crystal structures were obtained from RCSB PDB (inavolisib: 8EXV, taselisib: 8EXL, CH5132799: 3APC, alpelisib: 7MYO, ZSTK474: 2WXL). Subsequently, each structure was aligned to AlphaFold using PyMOL. The co-crystal structure of PI3K α was removed, leaving only the inhibitor structure in complex with AlphaFold. The same process was performed with the ATP-bound co-crystal structure (PDB: 1E8X).

Variables and measurements

The *in silico* exploratory assays included the following variables: FDA-approved drugs identified through virtual screening, binding energies (kcal/mol) obtained from molecular docking between the catalytic domain of PI3K and the screened drugs, and the amino acids of the drug-protein interaction.

For virtual screening, pharmacophores were generated using the Pharmit web server (<http://pharmit.csb.pitt.edu/>). Each pharmacophore was designed with five key positions, determined based on the most important inhibitor-protein interactions (inavolisib, taselisib, alpelisib, CH5132799 and ZSTK474) identified via the Protein-Ligand Interaction Profiler (PLIP) web tool (<https://plip-tool.biotech.tu-dresden.de/plip-web/plip/index>). This was further complemented by a literature review on the key regions and amino acids involved in the phosphorylation process between ATP and PI3K α . With this information, the key positions were defined and their XYZ coordinates were extracted using Pharmit and PyMOL. The virtual screening was conducted with the FDA-approved drug library. A tolerance of 0.5 was set in the “Receptor-Exclusive Shape” command to constraint the molecule size within the ATP-binding pocket.

Binding energies were calculated using the Yet Another Scientific Artificial Reality Application (YASARA) with the “BindEnergy” command. Prior to this, the structures were preprocessed with the “Clean” command and the missing hydrogens were added with the “AddHyd” command. A 10 Å box was generated around the system to encompass the entire protein, followed by energy minimization and docking. Drug-protein interaction amino acids were identified using the PLIP web tool.

Statistical analysis

Descriptive statistics were used to evaluate the binding affinity between the selected drugs and the catalytic domain of PI3K. The values were expressed in a bar graph to visualize the distribution of binding energies. In addition, the frequency of specific interactions was calculated for the selected drugs as candidates for drug repositioning.

Ethical considerations

This study was approved by the Institutional Research Ethics Committee at Universidad de Piura (Approval No. PREMEO820219). As an *in silico* study, it did not involve human participants or biological materials. The research was conducted in two laboratories at Universidad de Piura: Laboratorio de Cultivo Celular, Microbiología e Inmunología (Cell Culture, Microbiology and Immunology

Laboratory) and Laboratorio de Análisis de Proteínas y Bioinformática (Protein Analysis and Bioinformatics Laboratory).

RESULTS

Based on the interactions analysis and literature findings, this study proposes nine pharmacophore models (Table 1), each comprising five key features that reflect the most critical positions used by the existing inhibitors and ATP-binding regions in kinases ⁽¹²⁾. Pharmacophores 1, 2 and 3 include positions within the adenine and buried regions. Pharmacophores 4 and 5 incorporate positions in the solvent-accessible region, while pharmacophores 6 and 7 extend into the sugar pocket. Finally, pharmacophores 8 and 9 introduce positions in the phosphate-binding region.

Table 1. Pharmacophore models and their different characteristics

Model	Characteristics
Pharmacophore 1	HBA1, Hyd1, HBA2, Hyd2, HBA3
Pharmacophore 2	HBA1, Hyd1, HBA4, Hyd2, HBA3
Pharmacophore 3	HBA1, Hyd1, Hyd3, HBA5, HBA6
Pharmacophore 4	HBA1, Hyd1, HBD1, Hyd2, HBA3
Pharmacophore 5	HBA1, Hyd1, Hyd2, HBA3, HBA7
Pharmacophore 6	HBA1, Hyd1, Hyd2, HBA3, HBD2
Pharmacophore 7	HBA1, Hyd1, Hyd2, HBA3, HBA8
Pharmacophore 8	HBA1, Hyd1, Hyd2, HBA3, HBA9
Pharmacophore 9	HBA1, Hyd1, Hyd2, HBA3, HBA10

HBD: hydrogen bond donor; HBA: hydrogen bond acceptor; Hyd: hydrophobic; Aro: aromatic ring.

The generated pharmacophore models were used to screen for drugs containing these features in the FDA-approved drug library available in Pharmit. Initially, 33 drugs were identified across the nine proposed models (Table 2). To eliminate

redundancy, repeated drugs appearing in more than one pharmacophore model were evaluated based on their binding energy, and only the most relevant candidate was retained. This process resulted in a final selection of 22 drugs.

Table 2. Drugs identified from each model

Model	FDA-approved drugs
1	Sulfadoxine, cefonicid, apalutamide
2	Entecavir
3	Cefamandole, dexamethasone, sulfamethazine, terazosin, trazodone
4	Azilsartan, larotrectinib, regadenoson, sildenafil
5	Ceftazidime, entecavir, omeprazole, regadenoson, ritodrine, vardenafil
6	Nelarabine, riboflavin
7	Azelastine, bosentan, entecavir, fostamatinib, riboflavin, tenofovir
8	Fostamatinib, pralatrexate
9	Entecavir, nizatidine, pralatrexate, tedizolid

For each identified drug, the binding energy (kcal/mol) of the complex formed between PI3K and FDA-approved drugs was measured. The same analysis was conducted for known PI3K inhibitors (inavolisib, tasiselisib, CH5132799, alpelisib, ZSTK474) with PI3K (Figure 1A).

Among the FDA-approved drugs, pralatrexate (57.2 kcal/mol) and entecavir (56.1 kcal/mol) exhibited the highest binding energy to PI3K, surpassing most PI3K inhibitors (alpelisib: 53.28 kcal/mol, inavolisib: 53.13 kcal/mol, CH5132799: 43.31 kcal/mol, ZSTK474: 47.02 kcal/mol). Among the

existing PI3K α inhibitors, tasiselisib had the highest binding energy (59.75 kcal/mol), exceeding all other tested drugs.

The individual binding energy values of the FDA-approved drugs obtained through virtual screening were compared against the average binding of existing PI3K-specific inhibitors. Based on this comparison, 10 potential drug candidates were identified with binding energy values within a range of -10 to +10 (Figure 1B). Table 3 provides a detailed description of the binding characteristics of these 10 candidates for drug repositioning within the active site of PI3K α .

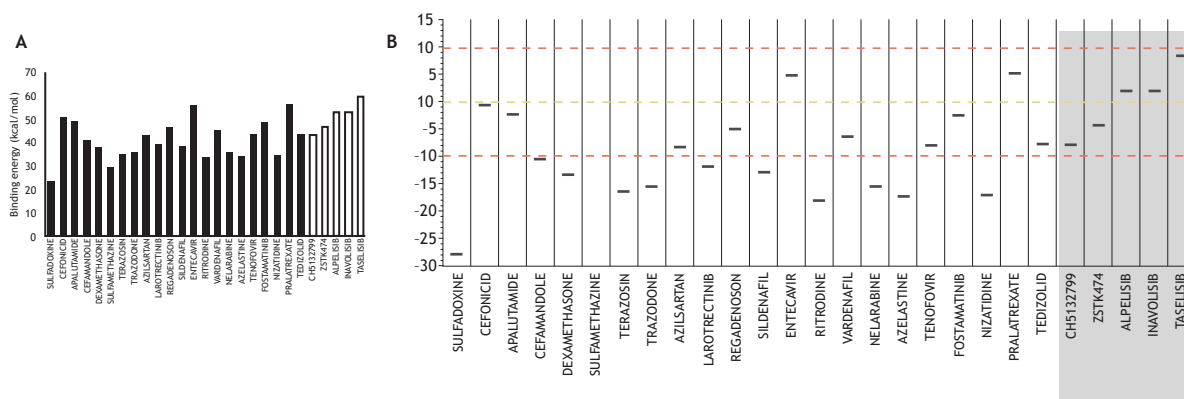


Figure 1. Binding energy between PI3K and tested drugs. (A) Black bars represent the binding energy of PI3K with FDA-approved drugs for other indications, whereas white bars represent the binding energy of PI3K with specific inhibitors. (B) Scatter plot of the binding energy between PI3K α and tested drugs. Drugs with binding energy within a range of -10 to +10 kcal/mol (indicated by red lines) were considered acceptable candidates. Existing PI3K α -specific inhibitors are shaded in gray.

Identification of PI3K α inhibitors through pharmacophore design
and drug repositioning

Table 3. Characteristics of candidates for drug repositioning

Drugs	Binding energy (kcal/mol)	Hydrogen bonds	Hydrophobic interactions	Pi stacking	Salt bridges
Fostamatinib	48.7	Arg770 His855 Gln859 Asp933	-	-	Arg770
Entecavir	56.1	Ser773 Ser774 Val851 Gln859 Ser919 Asp933	Ile800 Ile932	-	-
Pralatrexate	56.4	Ser774 Lys802 Asn853 Ser854 Gln859	Ile800 Tyr836 Val850 Val851 Ile932	-	-
Tedizolid	43.6	Asp810 Gln859 Asp933	Ile800 Ile848 Ile932	Trp780	Asp810 Asp933
Tenofovir	43.5	Asp810 Gln859 Asp933	Trp780 Ile800 Val850 Gln859	Trp780	-
Vardenafil	45	Arg770 Val851 Ser854 Gln859	Trp780 Ile800 Ile932	Trp780	-
Regadenoson	46.2	Val851 Ser854 Gln859 Asp933	-	-	-
Apalutamide	49	Val851 Ser854 His855 Gln859 Asp933	Trp780 Ile848 Val851 Phe930 Ile932	-	-
Cefonicide	50.6	Val851 Asn853 Ser854 His855 Gln859	Ile800 Tyr836 Ile848 Ile932	-	-
Azilsartan	42.9	Arg770 Gln859 Asp933	Ile800 Lys802 Tyr836 Ile848 Val851 Thr856 Ile932	-	Lys802

DISCUSSION

Out of the 10 abovementioned drugs, three in particular—fostamatinib, pralatrexate and entecavir—have been selected as potential candidates for drug repositioning based on their *in silico* interactions and studies exploring their possible use in cancer treatment.

Fostamatinib is an inhibitor of spleen tyrosine kinase (Syk), approved for the treatment of chronic autoimmune thrombocytopenia in patients who have failed conventional therapy⁽¹³⁾. However, its use is also being evaluated for other conditions⁽¹⁴⁾. Previous studies have identified Syk protein as a key molecular mediator in the regulation of epithelial-mesenchymal plasticity (EMP) and the epithelial-mesenchymal transition (EMT), an essential process in the development of metastasis from a primary tumor⁽¹⁵⁾. Although initial studies found lower Syk expression in cancer patient tissues—indicating a potential tumor suppressor role⁽¹⁶⁾—experimental research has shown that Syk directly participates in EMT and suggests that its inhibition—using fostamatinib, for example—could reduce the likelihood of metastasis^(15,17). At the clinical level, fostamatinib has shown mixed results in terms of tolerance and limited efficacy against certain solid tumors, indicating that the results remain inconclusive^(14,18). Its interaction with kinases other than Syk, such as Flt3, JAK, c-Kit, Lck and RET, has already been reported⁽¹⁴⁾, although its potential as a PI3K inhibitor has not yet been evaluated. In our *in silico* findings, fostamatinib interacts with PI3K by forming hydrogen bonds with His855, Gln859, Asp933 and Arg770, as shown in Figure 2A. These interactions are also observed in existing PI3K α inhibitors and ATP. Bonds with His855 and Gln859 residues could enhance specificity for PI3K α ⁽¹⁹⁾. Notably, the carboxamide of alpelisib, taselisib and inavolisib also binds to Gln859⁽²⁾, suggesting that this residue plays a key role in determining the affinity between PI3K α and other isoforms⁽¹⁹⁾. Asp933 is part of the conserved DFG (aspartate, phenylalanine and glycine) motif found in all protein kinases, which plays a critical role in catalysis by binding Mg²⁺ ion to orient the ATP γ -phosphate for transfer⁽²⁰⁾. This residue is also a common binding target of the aforementioned PI3K α inhibitors⁽²⁾.

On the other hand, pralatrexate is used to treat advanced or recurrent peripheral T-cell lymphoma. It is an antimetabolite inhibitor and folic acid analog that prevents DNA replication and disrupts the cell cycle.

Preclinical studies have shown promising results for pralatrexate in high-risk neuroblastoma, demonstrating superior efficacy compared to methotrexate⁽²¹⁾, as well as advantages over other antimetabolites in recurrent or refractory non-small cell lung cancer (NSCLC) and certain types of lymphomas⁽²²⁾. Moreover, pralatrexate has been proposed for repositioning in the treatment of COVID-19 due to its viral effects in addition to its antineoplastic properties⁽²³⁾. However, no studies have reported its effect on PI3K α kinase or cancers with a high mutation rate in this enzyme, making our findings potentially relevant for future applications. As illustrated in Figure 2B, pralatrexate interacts with PI3K α by binding not only to Gln85 but also to the catalytic residues Lys802 and Ser854. Lys802 is known to participate in the phosphate transfer reaction of p110 α ^(20,24,25) and serves as an interaction target for the PI3K α -specific inhibitor CH5132799⁽²⁾. Additionally, Ser854 has been reported to interact with alpelisib, taselisib and inavolisib⁽²⁾, indicating its importance as residue in the catalytic function of PI3K α .

Entecavir is a nucleoside antiviral that has been used for nearly two decades to treat chronic hepatitis B virus infection by inhibiting viral replication⁽²⁶⁾. As a guanine analog, its role in cancer therapy has been explored through *in silico* drug repositioning studies, suggesting its potential as a chemotherapeutic agent for breast, ovarian and prostate cancer, as well as in tissues with high PARP-1 activity^(27,28). However, its potential as an inhibitor of key kinases involved in cancer progression, such as PI3K α , has not been evaluated. As shown in Figure 2C, entecavir interacts with PI3K α similarly to fostamatinib, forming bonds with Gln859 and Asp933, which may confer the previously described characteristics. Additionally, it interacts with Val851, which is located in the kinase hinge region. This residue is also targeted by other known PI3K α inhibitors, including alpelisib, taselisib, inavolisib and CH5132799⁽²⁾.

Finally, it is worth highlighting that other drugs with promising *in silico* results against PI3K are already being tested for cancer therapy. One example is tenofovir, a drug used to treat HIV infection, which has demonstrated potential effects in certain types of recurrent or advanced cancers, such as hepatocellular carcinoma^(29,30).

Identification of PI3K α inhibitors through pharmacophore design and drug repositioning

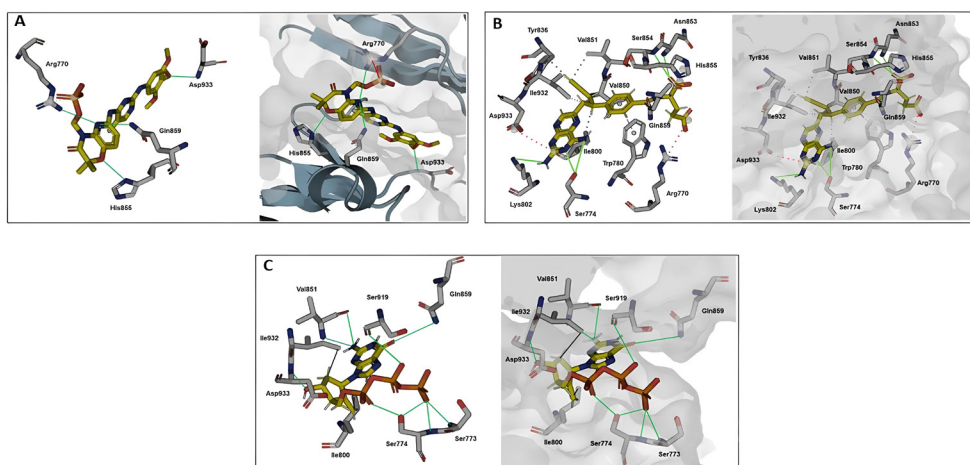


Figure 2. Drug-protein interaction. (A) Interaction between fostamatinib and PI3K. (B) Interaction between pralatrexate and PI3K. (C) Interaction between entecavir and PI3K. All interactions are shown in stick representation (left side of the panel) and surface representation (right side of each panel). Hydrogen bonds are represented by green lines.

In conclusion, this study identified 10 drugs with potential for repositioning in cancer treatment based on their interaction with PI3K α . Among these, fostamatinib, pralatrexate and entecavir were selected due to their in silico interactions and prior studies supporting their potential applications in cancer treatment. These drugs are currently being tested experimentally or are undergoing clinical trials, primarily targeting kinase proteins, which makes their interaction with PI3K α a viable possibility. Additionally, this project generated nine pharmacophores, which can be incorporated into specialized databases to facilitate the search for new molecules and/or drugs with potential for repositioning. Therefore, based on these findings, further in silico and in vitro research are recommended, focusing on their role in PI3K α inhibition and in neoplasms where this kinase's activity or mutations play a crucial role.

Acknowledgements: We extend our sincere gratitude to Dr. Silvia Suárez Cuzna from Instituto de Bioquímica y Nutrición (Institute of Biochemistry and Nutrition) "Alberto Guzmán Barrón" at Universidad Nacional Mayor de San Marcos for her insightful review and valuable comments on this article.

Author contributions: PWC, SIV and JFC conceptualized the study; PWC, DRL and JFC curated the data; and PWC, DRL, RZD and JFC utilized software for the analysis. Additionally, PWC, DRL, RZD, BMD and JFC conducted the formal analysis and research, while SIV and RZD secured funding from Consejo Nacional de Ciencia, Tecnología e Innovación (Concytec - National Council for Science, Technology and Innovation)-Programa Nacional de Investigación Científica y Estudios Avanzados (ProCiencia - National Program for Scientific Research and Advanced Studies). Data collection was carried out by PWC, DRL,

RZD and JFC. Furthermore, SIV, RZD and JFC designed the research methodology, and PWC and DRL drafted the original manuscript. All authors contributed to the writing, review and editing of the manuscript.

Funding sources: This research was funded by Concytec through ProCiencia, under the project entitled *Determinación in vitro de nuevas dianas terapéuticas en modelos celulares de cáncer de pulmón de células no pequeñas positivo para la mutación del gen linfoma anaplásico quinasa (ALK) resistente a inhibidores selectivos de la proteína ALK* (In vitro determination of new therapeutic targets in cellular models of non-small cell lung cancer positive for the anaplastic lymphoma kinase (ALK) gene mutation resistant to selective ALK protein inhibitors), contract number 375-2019-FONDECYT. Additionally, it was funded by Universidad de Piura, under project PI2106 entitled *Patrón metabólico y expresión de la vía PI3K/AKT en líneas celulares de cáncer de pulmón de células no pequeñas ALK+ resistentes a inhibidores de tirosina quinasa* (Metabolic pattern and expression of the PI3K/AKT pathway in ALK+ non-small cell lung cancer cell lines resistant to tyrosine kinase inhibitors).

Conflicts of interest: The authors declare no conflicts of interest.

BIBLIOGRAPHIC REFERENCES

1. Astudillo-de la Vega H, Ruiz-García E, Martínez-Cedillo J, Ochoa-Carrillo FJ. El papel de la quimiorresistencia en los tumores sólidos. *Gac Mex Oncol* [Internet]. 2010;9(3):117-26.
2. Vanhaesebroeck B, Perry MWD, Brown JR, André F, Okkenhaug K. PI3K inhibitors are finally coming of age. *Nat Rev Drug Discov* [Internet]. 2021;20(10):741-69.

3. Zhang Y, Kwok-Shing Ng P, Kucherlapati M, Chen F, Liu Y, Tsang YH, et al. A Pan-Cancer Proteogenomic Atlas of PI3K/AKT/mTOR Pathway Alterations. *Cancer Cell* [Internet]. 2017;31(6):820-32
4. Zhang M, Jang H, Nussinov R. PI3K inhibitors: review and new strategies. *Chem Sci* [Internet]. 2020;11(23):5855-65.
5. Hennessy BT, Smith DL, Ram PT, Lu Y, Mills GB. Exploiting the PI3K/AKT pathway for cancer drug discovery. *Nat Rev Drug Discov* [Internet]. 2005;4(12):988-1004.
6. Mishra R, Patel H, Alanazi S, Kilroy MK, Garrett JT. PI3K inhibitors in cancer: Clinical implications and adverse effects. *Int J Mol Sci* [Internet]. 2021;22(7):3464.
7. Arafeh R, Samuels Y. PIK3CA in cancer: The past 30 years. *Semin Cancer Biol* [Internet]. 2019;59:36-49.
8. Clarke PA, Workman P. Phosphatidylinositolide 3-kinase inhibitors: addressing questions of isoform selectivity and pharmacodynamic/predictive biomarkers in early clinical trials. *J Clin Oncol* [Internet]. 2012;30(3):331-3.
9. Wang Y, Kuramitsu Y, Baron B, Kitagawa T, Tokuda K, Akada J, et al. PI3K inhibitor LY294002, as opposed to wortmannin, enhances AKT phosphorylation in gemcitabine-resistant pancreatic cancer cells. *Int J Oncol* [Internet]. 2017;50(2):606-12.
10. Garbi SI, Zvelebil MJ, Shuttleworth SJ, Hancox T, Saghir N, Timms JF, et al. Exploring the specificity of the PI3K family inhibitor LY294002. *Biochem J* [Internet]. 2007;404(1):15-21.
11. Pushpakom S, Iorio F, Eyers PA, Escott KJ, Hopper S, Wells A, et al. Drug repurposing: progress, challenges and recommendations. *Nat Rev Drug Discov* [Internet]. 2019;18(1):41-58.
12. Vulpetti A, Bosotti R. Sequence and structural analysis of kinase ATP pocket residues. *Il Farm* [Internet]. 2004;59(10):759-65.
13. Bussel J, Arnold DM, Grossbard E, Mayer J, Treliński J, Homenda W, et al. Fostamatinib for the treatment of adult persistent and chronic immune thrombocytopenia: results of two phase 3, randomized, placebo-controlled trials. *Am J Hematol* [Internet]. 2018;93(7):921-30.
14. Park SR, Speranza G, Piekarczyk R, Wright JJ, Kinders RJ, Wang L, et al. A multi-histology trial of fostamatinib in patients with advanced colorectal, non-small cell lung, head and neck, thyroid, and renal cell carcinomas, and pheochromocytomas. *Cancer Chemother Pharmacol* [Internet]. 2013;71(4):981-90.
15. Shinde A, Hardy SD, Kim D, Akhand SS, Jolly MK, Wang WH, et al. Spleen tyrosine kinase-mediated autophagy is required for epithelial-mesenchymal plasticity and metastasis in breast cancer. *Cancer Res* [Internet]. 2019;79(8):1831-43.
16. Sung YM, Xu X, Sun J, Mueller D, Sentissi K, Johnson P, et al. Tumor suppressor function of Syk in human MCF10A in vitro and normal mouse mammary epithelium in vivo. *PLOS ONE* [Internet]. 2009;4(10):e7445.
17. Braselmann S, Taylor V, Zhao H, Wang S, Sylvain C, Baluom M, et al. R406, an orally available spleen tyrosine kinase inhibitor blocks fc receptor signaling and reduces immune complex-mediated inflammation. *J Pharmacol Exp Ther* [Internet]. 2006;319(3):998-1008.
18. Flinn IW, Bartlett NL, Blum KA, Ardeshta KM, LaCasce AS, Flowers CR, et al. A phase II trial to evaluate the efficacy of fostamatinib in patients with relapsed or refractory diffuse large B-cell lymphoma (DLBCL). *Eur J Cancer* [Internet]. 2016;54:11-7.
19. Heffron TP, Heald RA, Ndubaku C, Wei B, Augustin M, Do S, et al. The rational design of selective benzoxazepin inhibitors of the α -isoform of phosphoinositide 3-Kinase culminating in the identification of (S)-2-((2-(1-isopropyl-1H-1,2,4-triazol-5-yl)-5,6-dihydrobenzo[f]imidazo[1,2-d][1,4]oxazepin-9-yl)oxy)propanamide (GDC-0326). *J Med Chem* [Internet]. 2016;59(3):985-1002.
20. Maheshwari S, Miller MS, O'Meally R, Cole RN, Amzel LM, Gabelli SB. Kinetic and structural analyses reveal residues in phosphoinositide 3-kinase α that are critical for catalysis and substrate recognition. *J Biol Chem* [Internet]. 2017;292(33):13541-50.
21. Clark RA, Lee S, Qiao J, Chung DH. Preclinical evaluation of the anti-tumor activity of pralatrexate in high-risk neuroblastoma cells. *Oncotarget* [Internet]. 2020;11(32):3069-77.
22. Marchi E, O'Connor OA. Safety and efficacy of pralatrexate in the treatment of patients with relapsed or refractory peripheral T-cell lymphoma. *Ther Adv Hematol* [Internet]. 2012;3(4):227-35.
23. Bae JY, Lee GE, Park H, Cho J, Kim J, Lee J, et al. Antiviral efficacy of pralatrexate against SARS-CoV-2. *Biomol Ther (Seoul)* [Internet]. 2021;29(3):268-72.
24. Walker EH, Perisic O, Ried C, Stephens L, Williams RL. Structural insights into phosphoinositide 3-kinase catalysis and signalling. *Nature* [Internet]. 1999;402(6759):313-20.
25. Wymann MP, Bulgarelli-Leva G, Zvelebil MJ, Pirola L, Vanhaesebroeck B, Waterfield MD, et al. Wortmannin inactivates phosphoinositide 3-Kinase by covalent modification of Lys-802, a residue involved in the phosphate transfer reaction. *Mol Cell Biol* [Internet]. 1996;16(4):1722-33.
26. Robinson DM, Scott LJ, Plosker GL. Entecavir: a review of its use in chronic hepatitis B. *Drugs*. 2006;66(12):1605-22.
27. Sherin DR, Manojkumar TK. Exploring the selectivity of guanine scaffold in anticancer drug development by computational repurposing approach. *Sci Rep* [Internet]. 2021;11(1):16251.
28. Lourenço T, Vale N. Pharmacological efficacy of repurposing drugs in the treatment of prostate cancer. *Int J Mol Sci* [Internet]. 2023;24(4):4154.
29. Zhang M, Wang D, Liu H, Li H. Tenofovir decrease hepatocellular carcinoma recurrence in chronic hepatitis B patients after liver resection. *Infect Agent Cancer* [Internet]. 2018;13:19.
30. Brüning A, Burger P, Ginkelmaier A, Mylonas I. The HIV reverse transcriptase inhibitor tenofovir induces cell cycle arrest in human cancer cells. *Invest New Drugs* [Internet]. 2012;30(4):1389-95.

Corresponding author:

Juan Enrique Faya Castillo

Address: C. Mártir José Olaya 162, Miraflores 15074


Telephone: (01) 213 9600 extension 2239

E-mail: juan.faya@udep.edu.pe / paolo.wong@udep.edu.pe

Reception date: November 2, 2023

Evaluation date: January 11, 2024

Approval date: February 16, 2024

© The journal. A publication of Universidad de San Martín de Porres, Peru.  Creative Commons License. Open access article published under the terms of Creative Commons Attribution 4.0 International License (<http://creativecommons.org/licenses/by/4.0/>).

ORCID iDs

Paolo Wong Chero

Daniel Ramírez Lupuche

Richard Zapata Dongo


Brenda Moy Díaz

Stefany Infante Varillas

Juan Faya Castillo


 <https://orcid.org/0000-0001-7635-0347>

 <https://orcid.org/0009-0003-9685-0375>

 <https://orcid.org/0000-0001-7634-1029>

 <https://orcid.org/0009-0008-3055-975X>

 <https://orcid.org/0000-0002-3067-233X>

 <https://orcid.org/0000-0002-3408-7971>